

Nonlocal-density-functional theory of inhomogeneous electron gas: Metal surface

Ichiro Yamashita and Setsuo Ichimaru

Department of Physics, University of Tokyo, 7-3-1 Hongo, Bunkyo-ku, Tokyo 113, Japan

(Received 4 August 1983)

We develop a theoretical framework within the density-functional formalism in which the nonlocal character of the exchange and correlation potential is appropriately taken into account in the description of an inhomogeneous many-electron system near the metal surface. The proposed theoretical scheme is sufficiently simple so that the self-consistent calculations of the electron density and the associated surface quantities such as the surface energy and work function can be practically carried out; the validity and accuracy of the approximations introduced for the simplification are examined and ascertained with the aid of exact sum rules. In the process we derive a useful analytic expression for the radial distribution function of the electrons at metallic densities.

I. INTRODUCTION

Conduction electrons in metals and related substances form degenerate electron liquids. A series of microscopic formulations and variational calculations have been advanced recently^{1,2} to elucidate the nature of the many-body effects, such as the exchange- and Coulomb-induced correlations, involved in such an electron system. The density-functional formalism, developed by Hohenberg, Kohn, and Sham³⁻⁵ has then provided a powerful tool in analyzing the properties of an inhomogeneous electron system such as the metal surface and the atoms.

Lang and Kohn⁶⁻⁸ carried out a pioneering study of the metal surface in the density-functional formalism. They calculated the electron distribution across the surface in the jellium model of the metal where the exchange and correlation effects are treated with the local-density approximation (LDA). The values of the work function so computed showed a good overall agreement with the experimental values for various metals. The surface-energy calculation, while in fair agreement with experiments at low electron densities made a totally inadequate prediction—to the point of giving the wrong, negative sign—for higher-density metals such as Al. They corrected this inadequacy by taking an additional account of the discrete ion-lattice effects.

Across the metal surface, the electron distribution varies so steeply that the characteristic length associated with its variation is estimated to be of the order of an average interparticle spacing. The applicability of the LDA to such an inhomogeneous system thus constitutes a fundamental question that remains to be answered in the treatment of the electron distribution.

A number of investigators⁹⁻¹² considered an improvement over the LDA scheme by including those terms stemming from the density-gradient expansion. Basically this is a perturbation-theoretical calculation in which the density variation is assumed to be weak. Opinion about the usefulness of including those gradient corrections in the exchange and correlation functional has been divided, however. Ma and Brueckner⁹ found that for heavy atoms

the correlation energy due to the density-gradient expansion overestimates the necessary correction by about a factor of 5. Gupta and Singwi¹⁰ estimated that with the use of the first gradient correction the remaining error in the metal surface energy was only a few percent. Lau and Kohn,¹¹ and Perdew, Langreth, and Sahni,¹² demonstrated that the first density-gradient correction to the LDA gives no improvement to the surface energy and worsens the density profile.

Other investigators used various approximation schemes to treat the nonlocal-density functional. Langreth and Perdew,¹³ considering the surface energy in terms of fluctuations at various wavelengths, interpolated between the LDA, accurate in the short-wavelength limit, and the random-phase approximation in the long-wavelength limit. In the process they concluded that the LDA gave reasonable accuracy (better than 10%) for the surface energy. Gunnarsson, Jonson, and Lundqvist¹⁴ noted the importance of securing certain conservation properties in the nonlocal, exchange and correlation hole. The proposed approximation schemes, however, turned out to be fairly complex so that the self-consistent solution for the density distribution has not been obtained.

Recently, Sun, Li, Farjam, and Woo¹⁵ carried out a variational calculation of the metal surface problem in the jellium model through the method of the correlated basis function. Their surface-energy results differed significantly from those of the LDA calculation.

In light of those recent developments the purpose of the present paper is to develop a theoretical framework within the density-functional formalism in which the nonlocal character of the exchange and correlation potential may be accounted for, with good accuracy, in the treatment of an inhomogeneous many-electron system. We aim at making the theoretical scheme sufficiently simple so that the self-consistent calculations of the electron density and other surface quantities can be practically carried out. The validity and accuracy of the approximations introduced for the simplification will be carefully examined and assured with the aid of various sum rules and other general considerations.

The outline of the paper is as follows. In Sec. II we formulate the metal surface problem in terms of the density-functional theory. The proposed scheme of treating the nonlocal exchange and correlation potential is described in Sec. III. Sum rules and limiting behaviors of the pair correlation function are examined and its analytic expression is derived in Sec. IV; the expression will be of use for computational purposes. In Sec. V we investigate the validity and accuracy of the approximation schemes adopted for the description of the nonlocal exchange and correlation potential. In Sec. VI we present numerical results for the solution to the set of the self-consistent equations on the electron-density distribution and various surface quantities; those are compared with other theoretical and experimental results. Concluding remarks are made in Sec. VII. Some of the computational details are described in the Appendix.

II. DENSITY-FUNCTIONAL FORMALISM

In the jellium model of metal one assumes that the charge distribution of the crystalline ions may be replaced by the positive-charge background of average density $e\bar{n}$. The metallic surface may then be modeled by a semi-infinite distribution of uniform ionic density,

$$n_+(\vec{r}) = \begin{cases} \bar{n}, & x \leq 0 \\ 0, & x > 0. \end{cases} \quad (1)$$

A self-consistent distribution of conduction electrons, shown schematically in Fig. 1, would make an electric double layer in the vicinity of $x=0$. A dimensionless density parameter may then be defined as

$$r_s = (3/4\pi\bar{n})^{1/3} m e^2 / \hbar^2. \quad (2)$$

For simple metals, which we are concerned with here, this parameter takes on the values 2–6.

Following the density-functional formalism developed by Hohenberg and Kohn,³ we express the ground-state energy of N electrons under the action of the external potential $v(\vec{r})$ as a functional of the electron-density distribution $n(\vec{r})$ in such as inhomogeneous system,

$$E_v[n] = \int v(\vec{r})n(\vec{r})d\vec{r} + \frac{e^2}{2} \int \frac{n(\vec{r})n(\vec{r}')}{|\vec{r}-\vec{r}'|} d\vec{r}d\vec{r}' + T_s[n] + E_{xc}[n]. \quad (3)$$

Here, $T_s[n]$ refers to the kinetic energy of a noninteracting electron system of density distribution $n(\vec{r})$, and $E_{xc}[n]$ denotes the contribution of the remaining exchange and correlation energy. The distribution satisfies the normalization condition

$$\int n(\vec{r})d\vec{r} = N. \quad (4)$$

According to the self-consistent formulation of the density-functional theory by Kohn and Sham,⁴ one finds an exact density distribution through a solution to the following set of self-consistent equations:

$$\left[-\frac{\hbar^2}{2m} \nabla^2 + v_{\text{eff}}[n; \vec{r}] \right] \psi_i = \epsilon_i \psi_i, \quad (5)$$

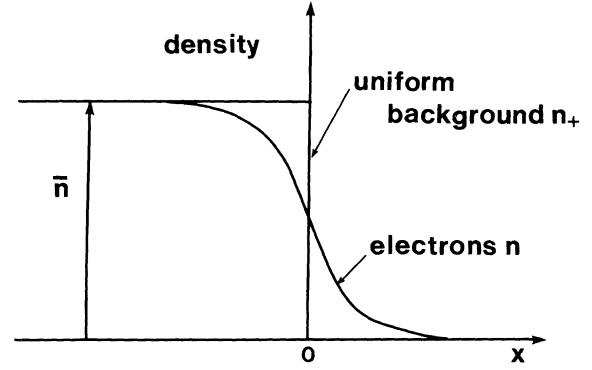


FIG. 1. Schematic view of density distributions.

$$n(\vec{r}) = \sum_{i=1}^N |\psi_i(\vec{r})|^2. \quad (6)$$

Here the ψ_i refer to those N electronic wave functions obtained as solutions to (5) with the lowest-energy eigenvalues ϵ_i , and the effective potential is defined as

$$v_{\text{eff}}[n; \vec{r}] = v(\vec{r}) + e^2 \int \frac{n(\vec{r}')}{|\vec{r}-\vec{r}'|} d\vec{r}' + v_{xc}[n; \vec{r}], \quad (7)$$

where the exchange and correlation potential is given by

$$v_{xc}[n; \vec{r}] = \frac{\delta E_{xc}[n]}{\delta n(\vec{r})}. \quad (8)$$

As Lang and Kohn⁶ have shown, the self-consistent equations mentioned above can be rewritten in the following form appropriate to the present surface problem:

$$\left[-\frac{\hbar^2}{2m} \frac{d^2}{dx^2} + v_{\text{eff}}[n; x] \right] \psi_k(x) = \left[\frac{\hbar^2}{2m} (k^2 - k_F^2) + \mu \right] \psi_k(x), \quad (9)$$

$$v_{\text{eff}}[n; x] = \phi[n; x] + v_{xc}[n; x] = -4\pi e^2 \int_x^\infty dx' \int_{x'}^\infty dx'' [n(x'') - n_+(x'')] + \phi(\infty) + v_{xc}[n; x], \quad (10)$$

$$n(x) = \frac{1}{\pi^2} \int_0^{k_F} dk (k_F^2 - k^2) [\psi_k(x)]^2, \quad (11)$$

where $k_F = (3\pi^2\bar{n})^{1/3}$ is the Fermi wave number in the interior of the metal. In Eq. (9), μ refers to the chemical potential,

$$\mu = \frac{\hbar^2 k_F^2}{2m} + \phi(-\infty) + v_{xc}[n; -\infty], \quad (12)$$

and the potential difference, $\Delta\phi \equiv \phi(\infty) - \phi(-\infty)$, is calculated as

$$\Delta\phi = 4\pi e^2 \int_{-\infty}^\infty x [n(x) - n_+(x)] dx. \quad (13)$$

III. NONLOCAL TREATMENT OF THE EXCHANGE AND CORRELATION POTENTIAL

The principal problem involved in the practical application of the density-functional formalism is how one estimates the exchange and correlation potential (8). Since the electron density is expected to exhibit a steep variation in the vicinity of the metal surface, nonlocality may play an essential role in the treatment of $v_{xc}[n; \vec{r}]$.

The LDA developed by Kohn and Sham⁴ and used for the surface problem by Lang and Kohn,^{6,7} however, assumes that the exchange and correlation energy is given by

$$E_{xc}[n] = \int \epsilon_{xc}[n(\vec{r})]n(\vec{r})d\vec{r}, \quad (14)$$

where $\epsilon_{xc}(n)$ refers to the exchange and correlation energy per particle for a homogeneous electron liquid with number density n . One can attempt to improve on the LDA by including those terms which systematically arise from the density-gradient expansion. Since the typical scale of the density variation is of the order of the average interparticle spacing ($\sim k_F^{-1}$), it is questionable if an inclusion of the first few terms in the gradient expansion would lead to a convergent and meaningful description of such a highly inhomogeneous system.

In this paper we wish to develop an alternative theoretical scheme by which the nonlocal character of the exchange and correlation potential may be appropriately taken into account even in a strongly inhomogeneous system, such as the electrons near the metal surface. The theory relies on adopting a certain functional form for the exchange and correlation energy functional $E_{xc}[n]$ whose validity and accuracy will be examined and ascertained in the light of sum rules in the inhomogeneous system.

We begin with an exact expression for the exchange and correlation energy functional,^{16,17}

$$E_{xc}[n] = \frac{1}{2} \int d\vec{r}d\vec{r}' \frac{n(\vec{r})n(\vec{r}')}{|\vec{r}-\vec{r}'|} \int_0^{e^2} d\alpha (g[\vec{r}, \vec{r}'; n] - 1). \quad (15)$$

Here $g[\vec{r}, \vec{r}'; n]$ is the pair distribution function of the system with a given electron-density distribution $n(\vec{r})$ and the Coulomb coupling constant α (equal to e^2); it is a symmetric two-point function of \vec{r} and \vec{r}' , and is a functional with respect to $n(\vec{r})$. For consideration of practical feasibility in carrying through the self-consistent calculation as exemplified in Eqs. (9)–(11), we approximate the pair distribution function of the inhomogeneous system by the radial distribution function of an equivalent homogeneous system with an average density n_{av} , so that

$$g[\vec{r}, \vec{r}'; n] \rightarrow g(|\vec{r}-\vec{r}'|, n_{av}). \quad (16)$$

Utility of the approximation scheme (16) rests on our ability to find an appropriate nonlocal-density dependence n_{av} sufficiently accurate to represent the inhomogeneous pair distribution. For reasons of symmetry and simplicity, we shall consider two such possibilities,¹⁸

$$n_{av} = \frac{1}{2}[n(\vec{r}) + n(\vec{r}')], \quad (17)$$

to be referred to as approximation scheme I, and

$$n_{av} = n\left(\frac{1}{2}(\vec{r} + \vec{r}')\right). \quad (18)$$

to be referred to as approximation scheme II. Later in Sec. V we shall examine and compare in detail the consequences of approximations (17) and (18) in light of exact sum rules and other considerations for the inhomogeneous system. We shall then find that assumptions (17) and (18) lead to markedly different predictions, scheme (17) being far superior for the description of the inhomogeneous electrons in the metal surface. It will also be shown that a third possible choice $n_{av} = [n(\vec{r})n(\vec{r}')]^{1/2}$, would behave analogously to Eq. (18) and therefore cannot be accepted.

We thus adopt (17) in (16) and calculate the exchange and correlation potential via (8). A nonlocal-density-functional theory of the surface electrons may thus be obtained by combining Eq. (8) self-consistently with the set of equations (9)–(11).

IV. ANALYTIC FORMULA FOR THE RADIAL DISTRIBUTION FUNCTION

To carry through the calculation for the solution of the self-consistent problem as described in the preceding section, one must find an analytic expression for the radial distribution function of the degenerate electron liquid at an arbitrary density which is simple and accurate enough for the use in numerical computations. In this section we shall derive such an expression, satisfying a number of exact boundary conditions and sum rules, and reproducing the results of the latest variational calculations.¹⁹

We begin by noting that the radial distribution function at short distances can be determined from the solution to the two-particle Schrödinger equation. Kimball²⁰ has thus shown the expansion

$$g(r) = g(0) + [g(0)/a_B]r + \dots, \quad (19)$$

where a_B is the Bohr radius. Yasuhara²¹ analyzed the short-range correlation through the consideration of electron-electron ladder diagrams, and thereby obtained an expression,

$$g(0) = \frac{1}{8}[z/I_1(z)]^2, \quad z = 4(\alpha r_s/\pi)^{1/2}, \quad (20)$$

where $I_1(z)$ is the modified Bessel function of first order, and $\alpha = (4/9\pi)^{1/3}$. Use of (20) in (19) thus enables one to determine the short-range values of $g(r)$.

For the long-range behavior, we take account of two sum rules. Firstly, the exchange and correlation energy $E_{xc}(r_s)$ per electron in rydbergs is directly related to the radial distribution function² via

$$\int_0^\infty dr r [g(r) - 1] = \frac{a_B^2}{3} r_s^2 \frac{d}{dr_s} [r_s^2 E_{xc}(r_s)]. \quad (21)$$

Secondly, we note that the depletion of electron density $n[g(r) - 1]$ around itself, i.e., the exchange-correlation hole, should contain a unit charge,

$$4\pi n \int_0^\infty dr r^2 [g(r) - 1] = -1. \quad (22)$$

For the exchange and correlation energy per particle of

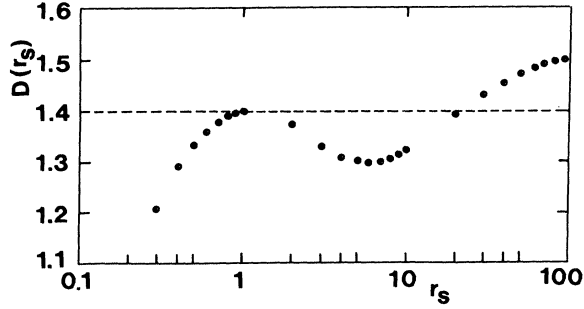


FIG. 2. Numerical solutions for $D(r_s)$. Dashed line represents Eq. (29); dots are the results of the numerical solution to Eq. (28).

the electron system in the paramagnetic state, we use the interpolation formula for the correlation energy,

$$E_c(r_s) = E_{xc}(r_s) + 0.916/r_s,$$

due to Vosko, Wilk, and Nusair,²²

$$r_s \frac{dE_c}{dr_s} = b_0 \frac{1 + b_1 y}{1 + b_1 y + b_2 y^2 + b_3 y^3}, \quad y \equiv \sqrt{r_s} \quad (23)$$

where $b_0 = 0.0621814$, $b_1 = 9.81379$, $b_2 = 2.82224$, and $b_3 = 0.736411$. Equation (23) is the Padé-approximant fitting to Ceperley and Alder's Monte Carlo data²³ on $E_c(r_s)$ at six values of r_s . We take Eqs. (21)–(23) to determine the long-range behavior of $g(r)$.

To accommodate boundary condition (19) and sum rules (21) and (22), we find it appropriate to express

$$g(r) = 1 + \left[A(r_s) + B(r_s) \frac{r}{r_0} + C(r_s) \frac{r^2}{r_0^2} \right] \times \exp \left[- \left[\frac{rD(r_s)}{r_0} \right]^2 \right]. \quad (24)$$

Here $r_0 = r_s a_B$,

$$A(r_s) = g(0) - 1, \quad (25)$$

$$B(r_s) = r_s g(0), \quad (26)$$

$$C(r_s) = \frac{2}{3[D(r_s)]^4} \frac{d}{dr_s} [r_s^2 E_{xc}(r_s)] - \frac{1}{[D(r_s)]^2} [g(0) - 1] - \frac{\pi^{1/2}}{2D(r_s)} r_s g(0), \quad (27)$$

and the parameter $D(r_s)$ is the solution to the quaternary equation,

$$\frac{8 - 3\pi}{16} r_s g(0) [D(r_s)]^4 - \frac{\pi^{1/2}}{8} [g(0) - 1] [D(r_s)]^3 + \frac{\pi^{1/2}}{4} \left[\frac{d}{dr_s} [r_s^2 E_{xc}(r_s)] \right] D(r_s) + \frac{1}{3} = 0. \quad (28)$$

Equations (25)–(27) are derived from (19) and (21); Eq. (28) is obtained by the use of (27) in (22).

As we find in Fig. 2, the solution to Eq. (28) yields the

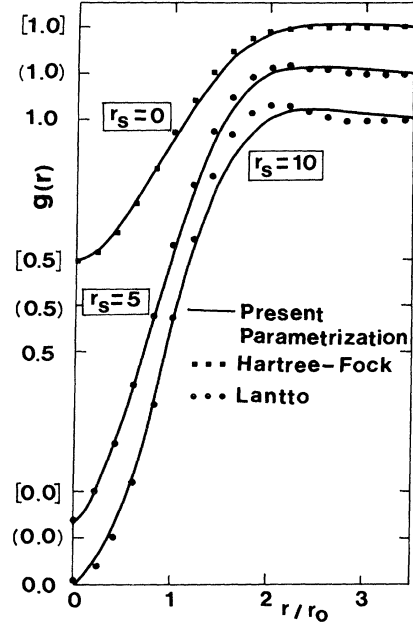


FIG. 3. Values of the parametrized formula Eq. (24) for the radial distribution function $g(r)$ at $r_s = 0, 5$, and 10 . Lantto refers to the data of Ref. 24.

values of the parameter $D(r_s)$ which remain almost constant over a wide range of r_s . Since a choice of a constant $D(r_s)$ facilitates the ensuing calculations substantially, we take

$$D(r_s) = 1.4, \quad (29)$$

with good accuracy. Use of (20), (23), and (29) in Eq. (24) through (25)–(27) completes the present parametrization for the radial distribution function.

In Fig. 3 we compare those parametrized values of $g(r)$ at $r_s = 0$ with the Hartree-Fock evaluation, and at $r_s = 5$ and 10 we do the same with Lantto's variational calculations on the basis of the Fermi-hypernetted-chain approximation.²⁴ We find that the agreement is satisfactory in the wide range of those r_s values.

V. APPROXIMATION SCHEMES OF THE NONLOCAL EXCHANGE AND CORRELATION POTENTIAL

In this section we take up the task of assessing explicitly the validity and accuracy of the nonlocal approximation schemes I and II introduced in Eq. (16) via Eqs. (17) and (18).

We begin by evaluating exchange and correlation potential (8) according to approximation schemes I and II; the electron-density distribution necessary for this evaluation is taken to be that obtained in the LDA by Lang and Kohn.⁶ The results are plotted in Fig. 4 at $r_s = 2$ and 5 . We note that $v_{xc}[x; n]$ in the metal interior ($x \leq 0$) agrees well in both evaluations. In the exterior ($x > 0$), however, $v_{xc}[x; n]$ in scheme II begins to diverge towards negative infinity as x increases, while $v_{xc}[x; n]$ in scheme I gradu-

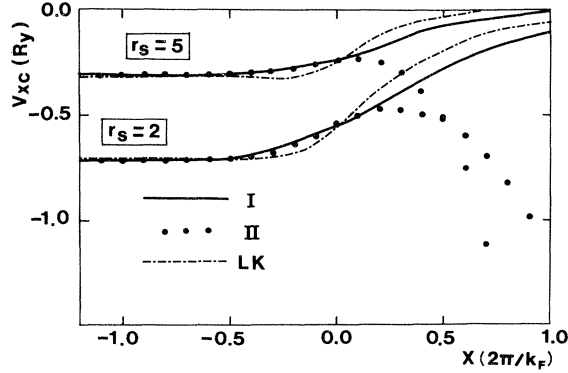


FIG. 4. Nonlocal exchange and correlation potential calculated in approximation schemes I and II [Eqs. (17) and (18)]. LK refers to the LDA values of Lang and Kohn (Ref. 6).

ally approaches the zero level, a tendency analogous to the image potential of the metal surface.

In scheme II, because of the negative divergence, it was, in fact, impossible to carry through the entire iterative calculations for the solution to the self-consistent equations. These features reflect a fatal flaw involved in approximation scheme II. In the following we demonstrate this defect first by a sum-rule argument and then through physical reasoning.

It is known⁵ that the inhomogeneous pair distribution function satisfies an exact sum rule,

$$\int n(\vec{r}') [g(\vec{r}, \vec{r}'; n) - 1] d\vec{r}' = -1, \quad (30)$$

the inhomogeneous counterpart to Eq. (22). Since we have adopted approximation (16), it is relevant to examine the values of the integral

$$J = \int n(\vec{r}') [g(|\vec{r} - \vec{r}'|, n_{av}) - 1] d\vec{r}'. \quad (31)$$

We have thus computed this integral at $r_s = 2$ and 5 in approximation schemes I and II with the electron-density distribution taken again from the LDA calculation. As we observe in Fig. 5, the computed values of J start with -1 in the metal interior and stay rather close to -1 even in the exterior domain for scheme I, while J in scheme II substantially deviates below -1 towards negative infinity for $x > 0$. It thus appears that approximation scheme I is inherently capable of sustaining the sum rule (30) for the inhomogeneous system.

A physical origin of these drastically different predictions between the schemes I and II may be traced as we recall sum rule (30) for an inhomogeneous system. Since $|g(\vec{r}, \vec{r}'; n) - 1|$ does not generally exceed unity, we note that the major contribution to sum rule (30) stems from the region where $n(\vec{r}')$ is large (i.e., the metal interior), and there $g(\vec{r}, \vec{r}'; n)$ would vanish roughly in the sub-domain $|\vec{r} - \vec{r}'| \leq [3/4\pi n(\vec{r}')]^{1/3}$. In approximation (16), $g(|\vec{r} - \vec{r}'|, n_{av})$ would likewise vanish within a radius, $r_{av} = (3/4\pi n_{av})^{1/3}$ as Eq. (22) indicates.

When both \vec{r} and \vec{r}' are located in the metal interior, inhomogeneity arising from the surface does not play an important part; schemes I and II would lead to an identi-

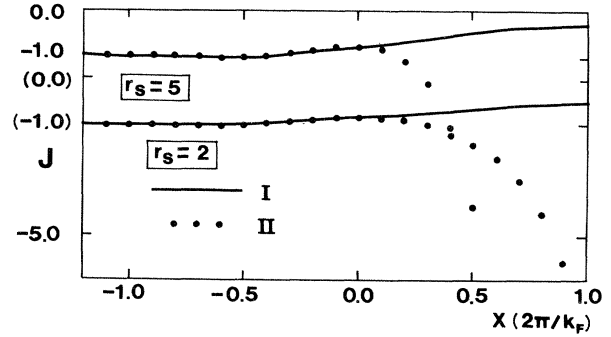


FIG. 5. Values of J , Eq. (31), according to approximation schemes I and II.

cal prediction since $n_{av} \simeq \bar{n}$ in either scheme. When \vec{r} is located outside the metal, however, the contribution to J arising from the \vec{r}' integration inside the metal differs diametrically in schemes I and II: In scheme I, we note

$$n_{av} = \frac{1}{2} [n(\vec{r}') + n(\vec{r})] \simeq \frac{1}{2} \bar{n}. \quad (32)$$

In scheme II, when $\frac{1}{2}(\vec{r} + \vec{r}')$ is located outside the metal, we find

$$n_{av} = n(\frac{1}{2}(\vec{r} + \vec{r}')) \simeq 0. \quad (33)$$

In the latter case, the range of the exchange and correlation hole would diverge; hence integral J would tend to diverge negatively as \vec{r} moves towards far outside the metal. It is clear that a third choice of n_{av} , such as $[n(\vec{r})n(\vec{r}')]^{1/2}$, would behave analogously to (33) and thus cannot be accepted.

The foregoing argument and examination have shown the validity and accuracy of the use of Eq. (17) in Eq. (16), i.e., scheme I, in approximating the nonlocal exchange and correlation potential (8). Although this scheme of evaluating $v_{xc}[n; x]$ may still contain a certain element of ambiguity in the far exterior of the metal, we expect that such an ambiguity should not cause much difference since the electron density itself is vanishingly small there. The validity of such an expectation is sustained as we find that the effective single-particle potential [Eq. (7)] calculated in scheme I closely resembles the classical image potential²⁵ far outside the metal surface.

To estimate numerically the degree of uncertainty involved in the evaluation of $v_{xc}[x; n]$ in the far exterior of the metal, we have carried out the following control calculations. Up to the point $x_m = 0.3(2\pi/k_F)$ at $r_s = 2$ or $x_m = 0.2(2\pi/k_F)$ at $r_s = 5$, where the integral J starts to exceed -1 , we use $v_{eff}[x; n]$, to be calculated self-consistently with scheme I in Sec. VI. For $x > x_m$, $v_{eff}[x; n]$ is matched to the image potential,²⁵

$$v_{image}(x) = -e^2/4(x - x_0), \quad (34)$$

with the effective position of the metal surface x_0 . The electron-density distribution thus obtained from Eq. (9) differs from the results obtained in Sec. VI only by 0.7% of \bar{n} .

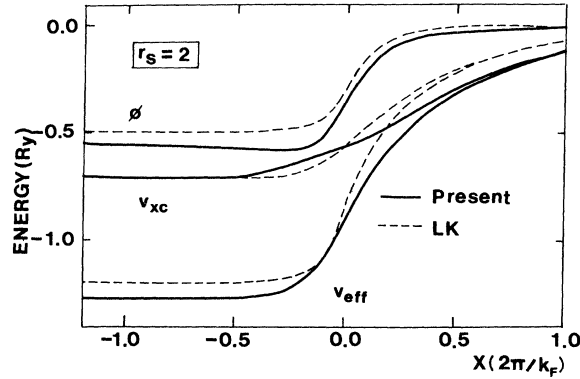


FIG. 6. Numerical results for the exchange and correlation potential $v_{xc}(x)$, the electrostatic potential $\phi(x)$, and the effective potential $v_{eff}(x)$ for $r_s=2$. LK refers to the LDA values of Lang and Kohn (Ref. 6).

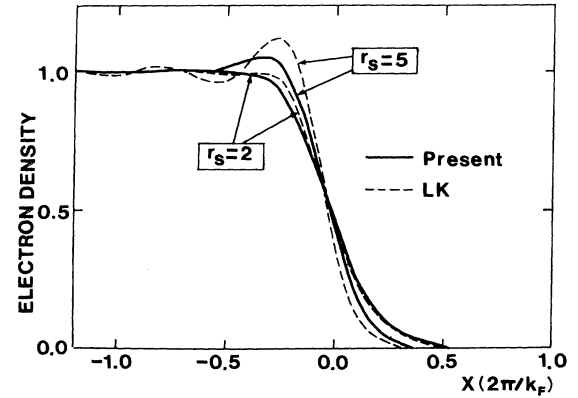


FIG. 7. Electron-density distributions in the surface region at $r_s=2$ and 5. LK refers to the LDA values of Lang and Kohn (Ref. 6).

VI. SELF-CONSISTENT CALCULATION AND NUMERICAL RESULTS

The long-range nature of the Coulomb potential makes a straightforward application of the iteration scheme to the self-consistent problem, Eqs. (5)–(8), rather unstable. To circumvent such an instability, Lang and Kohn⁶ devised a fairly complex method. In the present calculation we alternatively adopt the self-consistency procedure suggested by Nieminen²⁶ in his analysis of bimetallic systems. The outline of the procedure is described in the Appendix.

In Fig. 6 we plot the numerical results of the exchange and correlation potential $v_{xc}(x)$, the electrostatic potential $\phi(x)$, and the effective potential $v_{eff}(x)$ computed in the present scheme for the r_s value of 2; those are also compared with the LDA values obtained by Lang and Kohn.⁶ A notable feature in this comparison is the flattening of the exchange and correlation potential at the surface region, resulting from inclusion of the nonlocal effects.

Figure 7 shows computed results of the electron-density distribution at $r_s=2$ and 5; again a comparison is made with the LDA calculation.⁶ We thus find that the first peak inside the metal surface is lowered and broadened in the nonlocal treatment, a tendency analogous to the case of the surface potentials.

In Table I we list the computed values of the electrostatic dipole barrier $\Delta\phi$ of Eq. (13), and the work function,

$$\Phi = \Delta\phi - \left[\frac{\hbar^2 k_F^2}{2m} + v_{xc}[n; x = -\infty] \right]. \quad (35)$$

For comparison the LDA values⁷ are also listed. In Fig. 8 we compare the computed results of the work function with the LDA values and with the experimental values obtained for polycrystalline samples.²⁷ We observe in Fig. 8 that the present results, although staying somewhat above the LDA values, agree fairly well with the experimental values.

The surface energy, the energy required per unit area of a new surface formed by splitting a metal, can be written as a sum of three contributions,

$$\sigma = \sigma_s + \sigma_{xc} + \sigma_{es}, \quad (36)$$

with

$$\sigma_s = (2A)^{-1}(2T_s[n] - T_s[n']), \quad (37)$$

$$\sigma_{xc} = (2A)^{-1}(2E_{xc}[n] - E_{xc}[n']), \quad (38)$$

$$\sigma_{es} = (2A)^{-1}(2E_{es}[n] - E_{es}[n']). \quad (39)$$

Here A refers to the area of newly exposed face on each fragment, $n(\vec{r})$ and $n'(\vec{r})$ denote the density distributions for the split and unsplit metals, and $E_{es}[n]$ is the electrostatic energy defined and calculated as

TABLE I. Comparison of present values of the dipole barrier and the work function with the LDA values of Lang and Kohn (LK) in Ref. 7. Present results are obtained from Eq. (13). See the Appendix for the meaning of the numbers in the parentheses.

r_s	Dipole barrier (eV)		Work function (eV)	
	LK	Present	LK	Present
2	6.80	7.58	3.89	4.76(−0.34)
3	2.32	2.80	3.50	3.95(+0.23)
4	0.91	1.20	3.06	3.24(+0.11)
5	0.35	0.57	2.73	2.79(+0.06)
6	0.04	0.28	2.41	2.48(+0.02)

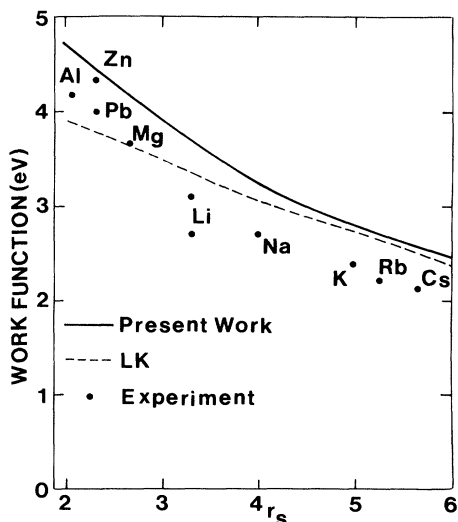


FIG. 8. Computed results (solid curve) of the work function compared with the LDA values (dashed curve) of Ref. 7, and the experimental values for polycrystalline metals.

$$E_{es}[n] = \frac{e^2}{2} \int d\vec{r}' d\vec{r} \frac{[n(\vec{r}) - \bar{n}][n(\vec{r}') - \bar{n}]}{|\vec{r} - \vec{r}'|}. \quad (40)$$

Table II lists the computed values of those surface energies and compares them with the LDA calculation of Lang and Kohn.⁶ Various theoretical evaluations of the total surface energy are plotted also in Fig. 9 together with the experimental values which are the linear extrapolations to zero temperature of measured liquid-metal surface tensions.²⁸ It is notable in Fig. 9 that the present nonlocal calculation for the jellium model follows the experimental data rather closely and stays positive even at higher densities, while the LDA (jellium) calculation by Lang and Kohn⁶ turns into negative for $r_s < 2.5$. The jellium calculation with the correlated basis functions by Sun, Li, Farjam, and Woo¹⁵ predicts the surface-energy values somewhere between the present nonlocal results and the LDA values. Those authors achieved an agreement with the experimental values by taking additional account of the cleavage energy and the local ion-pseudopotential contribution.

As we have just noted, the surface-energy values are quite sensitive to the ways in which one carries out its calculation even within the confines of the jellium model. It

is because the surface-energy calculation involves the detailed shapes of both the surface potential and the electron distribution. The work function, on the contrary, depends only on the far interior and exterior values of the potential, and so its value is not so sensitive to the fine details of the calculation.

Finally, we present another example illustrating such sensitivity by altering the magnitude of $D(r_s)$ used in Eq. (24): Instead of 1.4, we carry out the self-consistent calculation by choosing $D(r_s) = 1.3$ or 1.5, which may represent a lower or upper limit in the light of Fig. 2. The values of the work function computed at $r_s = 2$ and 5 by assuming $D(r_s) = 1.3$ or 1.5 are found to be almost identical to those with $D(r_s) = 1.4$; the work-function calculation is rather insensitive to a slight change of the value of $D(r_s)$ around 1.4. Analogous calculations for the surface energy are shown by the two dotted curves [upper: $D(r_s) = 1.3$; lower: $D(r_s) = 1.5$] in Fig. 9. Here the margin of uncertainty is considerable, especially for a high-density metal with $r_s < 3$.

VII. DISCUSSION AND CONCLUSION

We have presented a self-consistent calculation of the electron distribution and the associated quantities, such as the surface energy and the work function for a jellium model of metal surface, on the basis of a nonlocal-density-functional formalism. The nonlocality of the exchange and correlation potential has been taken into consideration through the use of the parametrized radial distribution function at an appropriately selected average density; the validity and accuracy of the approximation have been carefully examined.

The values of the work function and the surface energy computed in this scheme for the jellium model have shown an overall agreement with the experimental data obtained for real metals. The agreement on the work function may not be fortuitous, since its calculation does not involve the fine details of the electron distribution and of the potential.

We have also noted, through comparison with other theoretical calculations, that the predicted values of the surface energy can differ substantially from each other in the high-density domain ($r_s \leq 3.5$), even within the confines of the jellium model; the calculation of the surface energy depends critically on the detailed structure of the electron density. We do not, therefore, take the agreement between the present surface-energy calculation and experi-

TABLE II. Surface energy σ and its components in units of erg/cm². Present results are compared with the LDA results of Lang and Kohn (LK) in Ref. 6.

r_s	σ_s		σ_{xc}		σ_{es}		σ	
	LK	Present	LK	Present	LK	Present	LK	Present
2	-5600	-6100	3260	5800	1330	1700	-1010	1400
3	-720	-880	750	1600	170	270	200	970
4	-145	-220	260	620	45	75	160	480
5	-30	-70	115	300	15	30	100	260
6	-5	-25	55	170	10	15	60	160

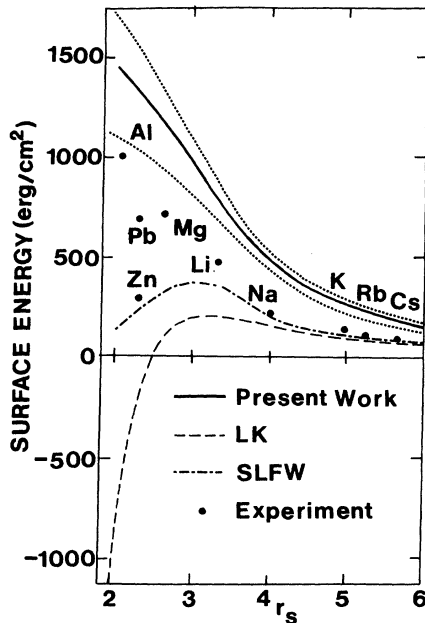


FIG. 9. Computed results (solid curve) of the surface energy in the jellium model compared with the LDA values of Lang and Kohn (LK) (Ref. 6), and the experimental values. SLFW refers to the values of Sun, Li, Farjam, and Woo (Ref. 15). See the text for the meaning of the two dotted curves.

ment on its face values, since the important pseudopotential corrections due to discrete ions have not been taken into account in the calculation.

In this connection we wish to comment on the agreement achieved between the experimental values of the metal-surface energy and the pseudopotential calculations by Lang and Kohn⁶ and by Sun, Li, Farjam, and Woo.¹⁵ Those authors first computed the surface energy for the jellium model, the results of which differed substantially from the experimental values; the computed results in some cases fell into negative domain. Therefore, a substantial margin of uncertainty still remains among various theoretical calculations of the surface energy in the jellium model.

The pseudopotential corrections were then computed perturbation theoretically with the use of the electron distribution obtained in the jellium model. It turned out that the resulting corrections were substantially large in magnitude; this would invalidate the perturbation-theoretical treatment.

As Fig. 6 of Ref. 6 would clearly illustrate, the magnitude and even the sign of such a correction depend sensitively on the fine structures of the electron distribution and the adopted pseudopotential. We thus remark that a large margin of uncertainty exists also in the calculation of the pseudopotential corrections. The excellent agreement between the experimental results and the pseudopotential calculations has been achieved through a delicate

balance between those considerable uncertainties involved both in the jellium calculation and in the pseudopotential correction.

It is in the sense as stated above that we still regard the jellium theory of the metal surface as containing open problems. The present study has been undertaken in the hope to reduce the range of uncertainty in the treatment of such a jellium model.

ACKNOWLEDGMENTS

We wish to thank H. Iyetomi and K. Utsumi for stimulating discussions on these and related subjects. The work was supported in part by the Japanese Ministry of Education, Science and Culture through Research Grants Nos. 56 380 001, 56 580 003, and 573 400 23.

APPENDIX: SELF-CONSISTENCY PROCEDURE

To overcome the numerical instability associated with the Coulomb potential, we follow the suggestion of Nieminen,²⁶ and recast the electrostatic potential in Eq. (10) into the form

$$\begin{aligned} \phi[n;x] = & \frac{1}{2q} \int_{x_1}^{x_2} dx' e^{-q|x-x'|} \\ & \times \{4\pi e^2 [n(x') - n_+(x')] + q^2 \phi[n;x']\} \\ & + C_1 e^{-q(x-x_1)} + C_2 e^{-q(x_2-x)}. \end{aligned} \quad (\text{A1})$$

Distant perturbations are screened out due to the exponential factor and the overall charge neutrality matters no more. Here the electrostatic potential appears in both sides of Eq. (A1) and we iterate Eqs. (9)–(11) and (A1) with respect to both the electron density and the electrostatic potential. The constants C_1 and C_2 are determined to satisfy the boundary conditions $\phi(x_1) = \phi(x_2) = 0$. As x_2 and x_1 , we take $2.0(2\pi/k_F)$ and $-4.0(2\pi/k_F)$; $q = (7/2\pi)k_F$ is adopted.

We prepare, as the trial electron density and the electrostatic potential, the form of Eqs. (2.7) and (2.8) in Ref. 29 and adjust the parameter β there until the fastest-converging procedure is obtained. It was essential to take as the input in each iteration a mixture of the input and output of the previous iteration.

Equation (A1) introduces a source of numerical error, because the electrostatic potential barrier calculated from the right-hand side of Eq. (13) may not be identical to $\phi[n;\infty] - \phi[n;-\infty]$ obtained directly from Eq. (A1). The difference between those two evaluations may thus be looked upon as an indication of errors inherent in the adoption of Eq. (1) for convergence. The values of the dipole barrier and the work function listed in Table I are those computed on the basis of Eq. (13). The work function calculated on the basis of Eq. (A1) can be obtained by the addition of the values in the parentheses to each result in Table I.

- ¹K. S. Singwi and M. P. Tosi, in *Solid State Physics*, edited by F. Seitz, D. Turnbull, and H. Eherenreich (Academic, New York, 1981), Vol. 36, p. 177.
- ²S. Ichimaru, *Rev. Mod. Phys.* **54**, 1017 (1982).
- ³P. Hohenberg and W. Kohn, *Phys. Rev.* **136**, B864 (1964).
- ⁴W. Kohn and L. J. Sham, *Phys. Rev.* **140**, A1133 (1965).
- ⁵W. Kohn and P. Vashishta, in *Theory of the Inhomogeneous Electron Gas (Physics of Solids and Liquids)*, edited by S. Lundqvist and N. H. March (Plenum, New York, 1983), p. 79.
- ⁶N. D. Lang and W. Kohn, *Phys. Rev. B* **1**, 4555 (1970).
- ⁷N. D. Lang and W. Kohn, *Phys. Rev. B* **3**, 1215 (1971).
- ⁸N. D. Lang, in *Solid State Physics*, edited by F. Seitz, D. Turnbull, and H. Eherenreich (Academic, New York, 1973), Vol. 28, p. 225.
- ⁹S. K. Ma and K. Brueckner, *Phys. Rev.* **165**, 18 (1968).
- ¹⁰A. K. Gupta and K. S. Singwi, *Phys. Rev. B* **15**, 1801 (1977).
- ¹¹K. H. Lau and W. Kohn, *J. Phys. Chem. Solids* **37**, 99 (1976).
- ¹²J. P. Perdew, D. C. Langreth, and V. Sahni, *Phys. Rev. Lett.* **38**, 1030 (1977).
- ¹³D. C. Langreth and J. P. Perdew, *Phys. Rev. B* **15**, 2884 (1977).
- ¹⁴O. Gunnarsson, M. Jonson, and B. I. Lundqvist, *Phys. Rev. B* **20**, 3136 (1979).
- ¹⁵Xin Sun, Tiecheng Li, Mani Farjam, and Chia-Wei Woo, *Phys. Rev. B* **27**, 3913 (1983).
- ¹⁶J. Harris and R. O. Jones, *J. Phys. F* **4**, 1170 (1974).
- ¹⁷O. Gunnarsson and B. I. Lundqvist, *Phys. Rev. B* **13**, 4274 (1976).
- ¹⁸Similar types of the nonlocal-density dependence have been discussed in the theory of classical liquid surface by C. Ebner, W. F. Saam, and D. Stroud, *Phys. Rev. A* **14**, 2264 (1976). A density dependence of (17) was assumed in a treatment of inhomogeneous density response by J. H. Rose and J. F. Dobson, *Solid State Commun.* **37**, 91 (1981); J. F. Dobson and G. H. Harris, *Phys. Rev. B* **27**, 6542 (1983).
- ¹⁹Parametrization of the electronic response functions in the same spirit has been carried out by S. Ichimaru and K. Utsumi, *Phys. Rev. B* **24**, 7385 (1981); K. Utsumi and S. Ichimaru, *Phys. Rev. A* **26**, 603 (1982); *Phys. Rev. B* **28**, 1792 (1983).
- ²⁰J. C. Kimball, *Phys. Rev. A* **7**, 1648 (1973).
- ²¹H. Yasuhara, *Solid State Commun.* **11**, 1481 (1972).
- ²²S. H. Vosko, L. Wilk, and M. Nusair, *Can. J. Phys.* **58**, 1200 (1980).
- ²³D. M. Ceperley and B. J. Alder, *Phys. Rev. Lett.* **45**, 566 (1980).
- ²⁴L. J. Lantto, *Phys. Rev. B* **22**, 1380 (1980), and private communication.
- ²⁵J. Bardeen, *Phys. Rev.* **58**, 727 (1940).
- ²⁶R. M. Nieminen, *J. Phys. F* **7**, 375 (1977).
- ²⁷Experimental data are taken from Table II of Ref. 7.
- ²⁸Experimental data are taken from Fig. 4 of Ref. 6.
- ²⁹J. R. Smith, *Phys. Rev.* **181**, 522 (1969).